PTEP

Prog. Theor. Exp. Phys. **2024** 101D01 (5 pages)
DOI: 10.1093/ptep/ptae155

Discovery of Neutron-Rich Silicon Isotopes ^{45,46}Si

Masahiro Yoshimoto*, Hiroshi Suzuki, Naoki Fukuda, Hiroyuki Takeda, Yohei Shimizu, Yoshiyuki Yanagisawa, Hiromi Sato, Kensuke Kusaka, Masao Ohtake, Koichi Yoshida, and Shin'ichiro Michimasa

RIKEN Nishina Center, RIKEN, 2-1 Hirosawa, Wako, Saitama 351-0198, Japan
*Email: masahiro.yoshimoto@riken.jp

Received September 3, 2024; Revised October 15, 2024; Accepted October 16, 2024; Published October 17, 2024

New isotopes ^{45,46}Si, which extend beyond the most neutron-rich Si isotopes confirmed thus far, have been discovered at the RI Beam Factory at the RIKEN Nishina Center. The isotopes were produced by the in-flight fragmentation reactions of ^{70}Zn at 345 MeV/nucleon on a Be target. All the projectile fragments were analyzed and identified using the large-acceptance two-stage separator BigRIPS. Consequently, six ^{45}Si events and one ^{46}Si event were confirmed. The neutron-bound nature of odd-N ^{45}Si may have a significant impact on the nuclear stability of neutron-rich proton *sd*-shell nuclei at approximately $N = 40$.

Subject Index D13, G12

1. Introduction. The diversity of atomic nuclei is a fundamental characteristic of matter and a critical factor influencing the properties of stars, the universe, and the existence of life. Therefore, the experimental determination of the boundary of nuclear existence on the proton–neutron plane is a key objective in nuclear physics. The neutron dripline, which is the boundary where an isotope can no longer hold additional neutrons, is an especially reliable benchmark to examine nuclear models. Consequently, it has a major impact on our understanding of nucleosynthesis.

Thus far, the neutron dripline has only been established up to Ne isotopes [1]. Several theoretical models have estimated the boundary beyond Ne isotopes, which have been optimized to reproduce the masses, half-lives, and excitation-level structures of as many known nuclei as possible [2]. However, these theoretical predictions for the dripline have not yet converged, resulting in low predictability. Therefore, direct observation of individual nuclei is the only reliable method to determine the boundary. At state-of-the-art radioactive-isotope (RI) beam facilities, experiments are being conducted to approach the theoretical neutron dripline, and the most neutron-rich isotopes from Na to Ca have been reported [3–6]. If we can experimentally determine whether neutron-rich isotopes of any of these elements are neutron-bound, the results will provide valuable insights into nuclear mass models and provide important data for estimating the neutron dripline of other elements in this region.

Recently, efforts to qualify the neutron dripline in this region have been reported based on the Bayesian regression of well cited global mass models [7] and ab initio calculations of nuclear structures in exotic nuclei [2]. According to evaluations by these studies, the posterior probabilities for ^{49}S and ^{52}Cl nuclei, which were first reported in Ref. [6], were 0.69 and 0.53 [7], and 0.90 and 0.78 [2], respectively. The bound nature in those odd-N nuclei im-

pacted the stability qualification of the Ca isotopes, with the estimated dripline extending to $N \sim 50$.

In neutron-rich Si isotopes, where the neutron-bound nature of isotopes up to $N = 29, 30$(^{43,44}Si [5,8]) has been confirmed, the same evaluations predicted the probabilities for ^{45}Si and ^{46}Si to be 0.60 and 0.94 [7], and 0.77 and 0.999 [2], respectively. The experimental confirmation of the bound properties of neutron-rich Si isotopes is considered indispensable for understanding nuclear stability, particularly in relation to nuclear deformation [9]. This letter reports our experimental research focusing on highly neutron-rich Si isotopes.

2. Experiment. The experiment was conducted at the RI Beam Factory (RIBF) [10] of the RIKEN Nishina Center. The primary beam consisted of ^{70}Zn ions with an energy of 345 MeV/nucleon, delivered by the cascade operation of the RIBF accelerator complex. The average intensity of the measurements was 600 particle-nA. Secondary RIs were produced by the projectile fragmentation process in a 10-mm-thick Be target, and were separated and analyzed in flight using the large-acceptance two-stage separator BigRIPS [11,12]. The magnetic rigidity of the first dipole magnet D1 was tuned to 6.6988 Tm to maximize the yield of the in-flight ^{45}Si fragments. The total momentum acceptance of the separator was set to 3% to effectively accept the fragments. To purify RIs around ^{45}Si, an Al achromatic degrader with a thickness of 5 mm was installed at the momentum-dispersive F1 focus of the first stage, with a horizontal slit set to $\pm$15 mm at the subsequent achromatic F2 focus.

To identify the RIs on an event-by-event basis, sets of two delay-line parallel-plate avalanche counters (PPACs) [13] for tracing ion trajectories and a thin plastic scintillator for hit timings were installed at the achromatic focal planes F3 and F7 and momentum-dispersive focal plane F5 of the second stage of the separator. An ionization chamber (IC) [14] was installed at the final focus F7 of the separator, which measured the energy deposits (ΔE) in the detector to identify the atomic numbers of the in-flight fragments. The particle identification (PID) of the fragments was analyzed using the acquired time of flight (TOF), magnetic rigidity ($B\rho$), and ΔE data. This PID scheme is called the TOF–ΔE–$B\rho$ method, and is described in detail in Ref. [15]. The TOF was measured over a 47-m flight path between achromatic foci F3 and F7. The $B\rho$ information for individual fragments was determined from trajectory measurements by the PPACs. Background events, such as signal pileups from light particles and reactions in the detectors, were rejected using correlations among hit positions and angles within the same focus as well as between different foci. In addition, a second Al achromatic degrader with a thickness of 3 mm was placed at F5 for identification of atomic numbers of fragments based on energy loss in the degrader [16,17]. Thus, the atomic numbers of the fragments in this measurement were determined by combining independent information from the IC and the second degrader. These careful analyses enabled reliable identification of a new isotope even with a single event.

3. Results and discussion. The PID plot obtained from the data analysis is shown in Fig. 1, where the total number of irradiated ^{70}Zn ions is 3.7×10^{17}. The horizontal and vertical axes represent the mass-to-charge ratio (A/q) and atomic number (Z), respectively. The observation of three events for ^{40}Mg and two events for ^{37}Na, along with the nonobservation of ^{39}Mg and ^{36}Na, is consistent with previously established neutron-bound properties [4,18]. The red solid

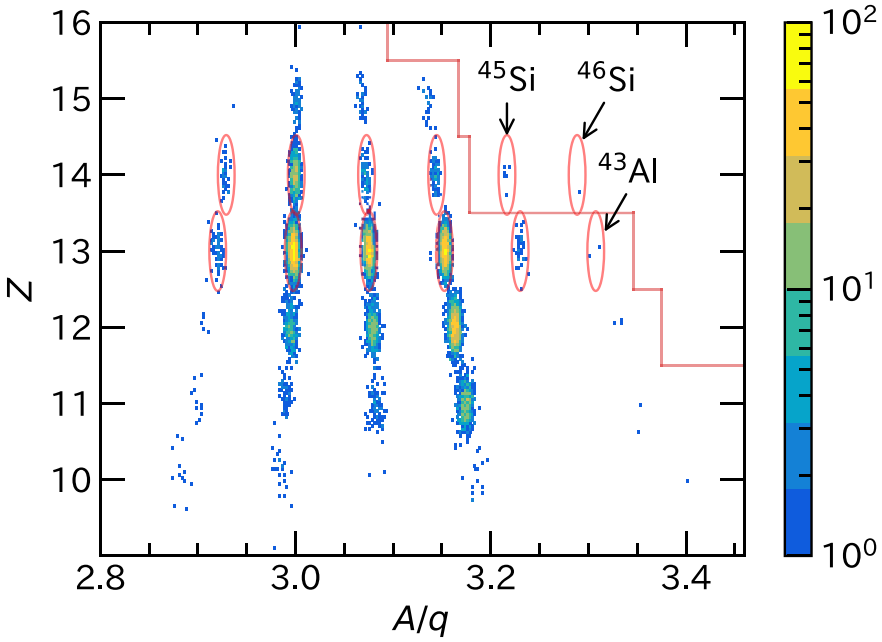

Fig. 1. Particle identification plot of projectile fragments produced by in-flight fragmentation reactions of ^{70}Zn at 345 MeV/nucleon on a Be target. The horizontal and vertical axes are the mass-to-charge ratio and atomic number of the detected fragments, respectively. The ellipses represent the 99% confidence interval for the isotopes based on the measured A/q and Z resolutions. The red solid line indicates the limit of known isotopes.

line indicates the limit of the known isotopes [3–6], and seven events were observed outside the limit of the Si isotopes. The fragments from Ne to P pass through the separator in a fully stripped ion state according to the evaluated transmission using LISE^{++} [19] under the present experimental conditions. Therefore, the A/q value is identical to A/Z. The absolute A/q resolution ($\sigma_{A/q}$) was 0.0028 and the absolute Z resolution (σ_Z) was 0.17, with the red ellipses representing the 99% confidence interval based on these resolutions. Six ^{45}Si candidates were clearly distinguished from the other isotopes. The A/q and Z values of a single ^{46}Si candidate was evaluated to determine whether it was a misidentification of ^{43}Al, the expected locus of which is closest to ^{46}Si in Fig. 1. The resultant χ^2 value for ^{43}Al was 52, with two degrees of freedom, yielding a p-value of much smaller than 0.01; thus, the possibility of ^{43}Al was significantly rejected. Finally, we conclude that six ^{45}Si particles and one ^{46}Si particle were observed in this experiment.

We examined the nuclear-bound nature of neutrons in ^{45,46}Si by comparing them with the findings of major theoretical mass models; the calculated one-neutron separation energies (S_{1n}) are listed in Table 1. The values shown on the AME2020 [20] line represent the evaluations based on this nuclear database. KTUY [21], HFB-24 [22], and FRDM(2012) [23] have been frequently cited for global nuclear mass predictions. WS4^{RBF} [24] and LZU [25] are theoretical predictions based on the macroscopic–microscopic Weizsäcker–Skyrme-type formula with two radial basis function (RBF) corrections. LZU (WS4^{RBF}) has been reported to reproduce the atomic masses listed in AME2016 (AME2012) with an accuracy of 149 keV (170 keV) in rms. UNEDF0 [26] is a global nuclear model based on a universal nuclear energy density functional that predicts the atomic masses and quadrupole deformation. UNEDF1 [27] is an updated version of UNEDF0, which adds the experimental excitation energies of the fission isomers in actinides to

Table 1. Predicted one-neutron separation energies (MeV) in ^{45,46}Si, ^{49}S, and ^{52}Cl. N/D indicates no information in the report of the model.

	^{45}Si	^{46}Si	^{49}S	^{52}Cl	Reproducibility
AME2020 [20]	0.29 ± 0.78	N/D	0.07 ± 0.30	0.00 ± 0.99	–
KTUY [21]	−0.43	1.76	−0.25	0.18	
HFB-24 [22]	−0.61	1.68	−0.21	−0.18	
FRDM(2012) [23]	−1.28	1.47	0.03	0.19	
WS4$^{\mathrm{RBF}}$ [24]	−0.21	1.62	−0.45	−0.85	
LZU [25]	0.94	1.32	0.49	−0.61	
UNEDF0 [26]	0.71	2.87	0.63	0.03	✓
UNEDF1 [27]	0.23	2.28	0.47	< 0	
DRHBc [28]	0.41	2.30	1.82	N/D	✓
VS-IMSRG [2]	0.43 ± 0.59	2.15 ± 0.59	0.77 ± 0.59	0.46 ± 0.59	✓

the list of fit observables. DRHBc [28] is a mass table in the deformed relativistic Hartree–Bogoliubov theory in a continuum with the PC-PK1 density functional established for even-Z nuclei. VS-IMSRG [2] is a microscopic calculation that uses the valence-space formulation of the in-medium similarity renormalization group.

The AME2020 evaluation indicated that all these odd-N nuclei were loosely bound; therefore, these isotopes were approaching the neutron dripline. We verified the reproducibility of these models based on the sign of S_{1n}, which indicates whether a valence neutron in the nucleus of interest is bound. The UNEDF0, DRHBc, and VS-IMSRG models successfully reproduced the bound nature of ^{45,46}Si, ^{49}S, and ^{52}Cl. UNEDF0 (DRHBc) calculations predict that the last neutron-bound Si isotope is ^{48}Si (^{52}Si), whereas ^{47}Si is (^{49,51}Si are) neutron-unbound. VS-IMSRG predicts that ^{48}Si is most likely to be located in the dripline, with the neutron-bound nature of ^{47}Si being evaluated at approximately 50%. Therefore, based on the results of this experiment, the neutron dripline nucleus of Si was considered to be at least ^{48}Si. In addition, investigating the nuclear stability of ^{47}Si is evidently essential for determining the location of the neutron dripline in Si isotopes. The neutron driplines of Ar isotopes predicted by UNEDF0, DRHBc, and VS-IMSRG were $^{58}_{18}\mathrm{Ar}_{40}$, $^{70}_{18}\mathrm{Ar}_{52}$, and $^{56}_{18}\mathrm{Ar}_{38}$, respectively. Therefore, the stability of ^{47}Si could help predict whether the Ar nuclei could hop over the $N = 40$ subshell closure.

4. Summary. In summary, we investigated the stability of the most neutron-rich Si isotopes ^{45,46}Si through experimental production using the BigRIPS separator at the RIKEN RI Beam Factory. We observed six events for ^{45}Si and one event for ^{46}Si. Because the data analysis showed that the probability of contamination of one ^{46}Si event by other known nuclei was extremely low, we concluded that ^{45,46}Si particles were particle-bound. These results provide important information for improving nuclear mass models and systematic estimates of the neutron-bound limit of the nuclear landscape, leading to the rejection of several existing models. In addition to the neutron-bound nature of the odd-N ^{45}Si nucleus revealed in this study, ^{47}Si is also considered a critical nucleus for estimating the neutron dripline of Si isotopes. This information may be useful for predicting the degree to which nuclear stability extends beyond neutron shell closures in heavier isotopes, such as those of Ar.

Acknowledgments

This experiment was conducted at the RIBF operated by the RIKEN Nishina Center and the Center for Nuclear Study, University of Tokyo. The authors thank the RIBF accelerator crew for providing the intense ^{70}Zn beam.

References

[1] D. S. Ahn et al., Phys. Rev. Lett. **123**, 212501 (2019).
[2] S. R. Stroberg, J. D. Holt, A. Schwenk, and J. Simonis, Phys. Rev. Lett. **126**, 022501 (2021).
[3] D. S. Ahn et al., Phys. Rev. Lett. **129**, 212502 (2022).
[4] T. Baumann et al., Nature **449**, 1022 (2007).
[5] O. B. Tarasov et al., Phys. Rev. C **75**, 064613 (2007).
[6] O. B. Tarasov et al., Phys. Rev. Lett. **121**, 022501 (2018).
[7] L. Neufcourt, Y. Cao, W. Nazarewicz, E. Olsen, and F. Viens, Phys. Rev. Lett. **122**, 062502 (2019).
[8] M. Notani et al., Phys. Lett. B **542**, 49 (2002).
[9] N. Tsunoda, T. Otsuka, K. Takayanagi, N. Shimizu, T. Suzuki, Y. Utsuno, S. Yoshida, and H. Ueno, Nature **587**, 66 (2020).
[10] Y. Yano, Nucl. Instrum. Meth. B **261**, 1009 (2007).
[11] T. Kubo, Nucl. Instrum. Meth. B **204**, 97 (2003).
[12] T. Kubo et al., Prog. Theor. Exp. Phys. **2012**, 03C003 (2012).
[13] H. Kumagai, T. Ohnishi, N. Fukuda, H. Takeda, D. Kameda, N. Inabe, K. Yoshida, and T. Kubo, Nucl. Instrum. Meth. B **317**, 717 (2013).
[14] K. Kimura et al., Nucl. Instrum. Meth. A **538**, 608 (2005).
[15] N. Fukuda, T. Kubo, T. Ohnishi, N. Inabe, H. Takeda, D. Kameda, and H. Suzuki, Nucl. Instrum. Meth. B **317**, 323 (2013).
[16] N. Fukuda et al., J. Phys. Soc. Jpn. **87**, 014202 (2018).
[17] Y. Shimizu et al., J. Phys. Soc. Jpn. **87**, 014203 (2018).
[18] M. Notani et al., Phys. Lett. B **542**, 49 (2002).
[19] O. B. Tarasov, D. Bazin, M. Hausmann, M. P. Kuchera, P. N. Ostroumov, M. Portillo, B. M. Sherrill, K. V. Tarasova, and T. Zhang, Nucl. Instrum. Meth. B **541**, 4 (2023).
[20] M. Wang, W. J. Huang, F. G. Kondev, G. Audi, and S. Naimi, Chin. Phys. C **45**, 030003 (2021).
[21] H. Koura, T. Tachibana, M. Uno, and M. Yamada, Prog. Theor. Phys. **113**, 305 (2005).
[22] S. Goriely, N. Chamel, and J. M. Pearson, Phys. Rev. C **88**, 024308 (2013).
[23] P. Möller, A. J. Sierk, T. Ichikawa, and H. Sagawa, At. Data Nucl. Data Tables, **109–110**, 1 (2016).
[24] N. Wang, M. Liu, X. Wu, and J. Meng, Phys. Lett. B **734**, 215 (2014).
[25] N.-N. Ma, H.-F. Zhang, X.-J. Bao, and H.-F. Zhang, Chin. Phys. C **43**, 044105 (2019).
[26] M. Kortelainen, T. Lesinski, J. Moré, W. Nazarewicz, J. Sarich, N. Schunck, M.V. Stoitsov, and S. Wild, Phys. Rev. C **82**, 024313 (2010).
[27] M. Kortelainen, J. McDonnell, W. Nazarewicz, P.-G. Reinhard, J. Sarich, N. Schunck, M.V. Stoitsov, and S.M. Wild, Phys. Rev. C **85**, 024304 (2012).
[28] P. Gao et al., At. Data Nucl. Data Tables **158**, 101661 (2024).